




## Excited-State OH Masers in the Water Fountain Source IRAS 18460–0151

XU-JIA OUYANG <sup>1</sup> YONG ZHANG <sup>1,2</sup> JUAN LI <sup>3,4</sup> JUN-ICHI NAKASHIMA <sup>1,2</sup> XI CHEN <sup>5,6</sup>  
 AND HAI-HUA QIAO <sup>7,8</sup>

<sup>1</sup>*School of Physics and Astronomy, Sun Yat-sen University, 2 Daxue Road, Tangjia, Zhuhai, Guangdong Province, China*

<sup>2</sup>*CSST Science Center for the Guangdong-Hongkong-Macau Greater Bay Area, Sun Yat-Sen University, Guangdong Province, China*

<sup>3</sup>*Department of Radio Science and Technology, Shanghai Astronomical observatory, 80 Nandan RD, Shanghai 200030, China*

<sup>4</sup>*Key Laboratory of Radio Astronomy, Chinese Academy of Sciences, China*

<sup>5</sup>*Center for Astrophysics, Guangzhou University, Guangzhou 510006, China*

<sup>6</sup>*Shanghai Astronomical Observatory, Chinese Academy of Sciences, 80 Nandan Road, Shanghai 200030*

<sup>7</sup>*National Time Service Center, Chinese Academy of Sciences, Xi'An, Shaanxi 710600, People's Republic of China*

<sup>8</sup>*Key Laboratory of Time Reference and Applications, Chinese Academy of Sciences, China*

### ABSTRACT

Water fountain objects are generally defined as “evolved stars with low to intermediate initial mass accompanied by high-velocity molecular jets detectable in the 22.235 GHz H<sub>2</sub>O maser line”. They are the key objects of understanding the morphological transitions of circumstellar envelopes during the post asymptotic giant branch phase. Masers are useful tools to trace the kinematic environments of the circumstellar envelopes. In this letter we report the discovery of exceptionally uncommon excited-state hydroxyl (ex-OH) masers at 4660 and 6031 MHz toward the water fountain source

IRAS 18460–0151. These are the brightest ex-OH masers discovered in late-type objects to date. To the best of our knowledge, prior to the current work, no evolved stellar object has been observed in the 4660 MHz ex-OH maser line. The ground-state hydroxyl (g-OH) masers at 1612 and 1665 MHz are also observed. The velocity components of the 4660 MHz ex-OH maser line and the much weaker 1665 MHz g-OH maser line all can be seen in the 1612 MHz g-OH maser line profile. The blue-shifted components of the three masers are more intense than the red-shifted ones, in contrast to the ex-OH maser line at 6031 MHz. The relevance of the behaviors of the ex-OH masers to the circumstellar environments is unclear.

*Keywords:* Astrophysical masers (103); Hydroxyl masers (771); Water masers (1790); Asymptotic giant branch stars (2100); Circumstellar masers (240)

## 1. INTRODUCTION

During their late evolutionary stage, low and intermediate mass stars ( $0.8\text{--}8 M_{\odot}$ ) will evolve to an asymptotic giant branch (AGB) phase, at which phase the star becomes incredibly unstable, with material flowing out and accumulating around the star to form a circumstellar envelope (CSE). The spherically symmetric CSE may transition into a bipolar or multipolar nebula after a short proto-planetary nebula (proto-PNe) period with a timescale of  $\sim 10^2\text{--}10^4$  yr (e.g., Kwok 1993; Ueta et al. 2000; Gledhill et al. 2001; Gómez et al. 2016). Despite years of intensive studies (e.g., Sahai & Trauger 1998), it remains unclear how the PNe are shaped. Many processes have been proposed to generate the bipolar morphology. A widely accepted scenario is that a common envelope developed by the binary interaction produces a high pole-to-equator density contrast which interacts with the subsequent fast wind to form the bipolar shaped nebulae (Livio & Soker 1988). Apart from that, magnetic fields might play some role on affecting the mass-loss rate, sculpting the stellar wind, and aligning the outflows (e.g., Falceta-Gonçalves & Jatenco-Pereira 2002; Frank & Blackman 2004; Nordhaus & Blackman 2006; Tocknell et al. 2014; Balick et al. 2020). However, it is unclear how

magnetic fields are generated and change during the evolution from the AGB to proto-PN to PN stages.

One of the primary approaches of measuring the magnetic field in evolved stars is the polarization measurement of masers (e.g., [Vlemmings 2014](#)). Ground-state OH masers (g-OH; 1.6–1.7 GHz), water masers (22.2 GHz), and SiO masers (43.1 GHz) have been commonly discovered in oxygen-rich AGB CSEs, which have been considered as crucial tracers of nebular conditions. Comparing the spatial distribution of the SiO maser spots and the orientation of the magnetic field in an OH/IR star, [Amiri et al. \(2012\)](#) concluded that the stellar outflow was shaped and defined by a dipole magnetic field.

“Water fountain” stars (WFs) are evolved stars equipped with high-velocity water masers (see [Imai 2007](#); [Desmurs 2012](#), for reviews). Their water maser spectra have a typical velocity spread of  $\geq 100 \text{ km s}^{-1}$  and a maximum velocity spread of  $\simeq 500 \text{ km s}^{-1}$  ([Gómez et al. 2011](#)). Thus far, 15 WFs have been found by interferometry measurements ([Desmurs 2012](#); [Gómez et al. 2017](#)). The spatiokinematics of the water masers of the WFs exhibit a broad diversity ([Imai et al. 2020](#); [Uscanga et al. 2023](#)). Given the short dynamical timescales of maser jets (5–100 yr; [Imai 2007](#); [Tafoya et al. 2020](#); [Imai et al. 2023](#)) and high optical obscuration ([Suárez et al. 2008](#)), WFs are likely to be in a transient phase between the AGB and proto-PN periods ([Khouri et al. 2021](#)). Consequently, WFs could be one of the first manifestation of collimated mass-loss in evolved stars, and thus are important objects for determining the timing and mechanisms of the disruption of spherical symmetry of the CSE.

The strength and direction of the in-situ magnetic fields in WFs could be measured in terms of the OH masers. As higher column densities are required for the inversion of the ex-OH line ([Cragg et al. 2002](#); [Wardle 2007](#)), g- and ex-OH masers are able to trace the magnetic fields at different circumstellar locations. However, there have been very few observations of ex-OH masers in CSEs ([Habing 1996](#)). Unambiguous detections include the 4765 MHz maser line in CRL 618 ([Strack et al. 2019](#)) and the 6035 MHz maser line in Vy 2-2 and K 3-35 ([Desmurs et al. 2010](#)). Less confident detections of the 4751 MHz maser line in AU Gem and the 6031 and 6035 MHz lines in NML Cyg have been reported ([Zuckerman et al. 1972](#); [Claussen & Fix 1981](#)), which were not confirmed by

subsequent observations probably due to either time variation in intensity or false signal (Sjouwerman et al. 2007, and references therein). In this letter, we report the first detection of ex-OH masers toward a oxygen-rich object IRAS 18460–0151 (I18460 hereafter).

I18460, firstly identified as a WF source by Deguchi et al. (2007), is a poorly studied target. It does not manifest radio continuum emission at 6 cm (Herman et al. 1985). Its water maser spectrum shows a velocity spread of  $\sim 290 \text{ km s}^{-1}$  with a central velocity of  $\sim 100 \text{ km s}^{-1}$ , while the CO ( $J = 1 - 0$  and  $J = 2 - 1$ ) lines peak at  $\sim 125 \text{ km s}^{-1}$  (Rizzo et al. 2013). The g-OH maser at 1612 MHz exhibits two peaks (Sevenster et al. 1997) with velocities at 111 and  $138.3 \text{ km s}^{-1}$ . The SiO  $J = 1 - 0$  and  $J = 2 - 1$  transitions were not detected (Deguchi et al. 2007). Recent observations of CO  $J = 2 - 1$  and  $\text{C}^{18}\text{O}$   $J = 2 - 1$  by the Atacama Large Millimeter/submillimeter Array (ALMA) indicate a lifetime of 150 years for the envelope (Khouri et al. 2021).

## 2. OBSERVATIONS AND DATA REDUCTION

The observations were performed at the Tianma 65-m Radio Telescope (TMRT), operated by Shanghai Astronomical Observatory, in the ‘position switching’ mode with an OFF position displaced by  $0.5^\circ$  in right ascension. The pointing position was R.A. =  $18^{\text{h}}48^{\text{m}}43^{\text{s}}.02$ , decl. =  $-01^\circ48'30''.2$  (J2000). The cryogenically cooled L/C/K band receivers were utilized for the observations of OH and water masers. The Digital Backend System was used to record signals in the left-hand circular polarization (LCP) and the right-hand circular polarization (RCP), simultaneously (Li et al. 2016). The signal of noise diodes was injected for the flux calibration. The calibration uncertainty is estimated to be within 30%.

The L-band observations were performed on December 16th and 18th 2023 with an integrated time of 20 minutes each. For the backend, Mode 24, which provides a bandwidth of 23.44 MHz in 65,536 channels, was used to record the OH masers at 1612, 1665, 1667, and 1720 MHz at four individual spectral windows. The velocity resolution is  $\sim 0.08 \text{ km s}^{-1}$  at 1.6 GHz. The aperture efficiency of the telescope is  $\sim 55\%$ , corresponding to a sensitivity of  $\sim 1.5 \text{ Jy K}^{-1}$ . The system temperature is about 20–30 K. The half-power beamwidth (HPBW) is  $\sim 10'$  at 1.6 GHz.

We carried out the C-band observations on December 10th, 16th, and 18th 2023 with an integrated time of 32, 20, and 64 minutes, respectively. Mode 24 of the backend was used, allowing to simultaneously cover the seven ex-OH transition lines at 4660, 4751, 4766, 6017, 6031, 6035, and 6049 MHz. The velocity resolution is  $\sim 0.02 \text{ km s}^{-1}$  at 6.0 GHz. In order to improve the signal-to-noise ratio, the spectra covering the ex-OH maser at 6031 MHz were smoothed to reduce the resolution to  $0.07 \text{ km s}^{-1}$ . The aperture efficiency of the telescope, the sensitivity, and the system temperature are the same as those of L-band observations. The HPBW is  $\sim 2'.6$  at 6.0 GHz.

The K-band observations were conducted on 2023 December 18 with an integration time of 16 minutes. The spectrum was recorded using Mode 20, which provides a bandwidth of 23.44 MHz in 4096 channels, resulting in a velocity resolution of  $0.08 \text{ km s}^{-1}$  at 22 GHz. The aperture efficiency was about 50%, corresponding to a sensitivity of  $\sim 1.7 \text{ Jy K}^{-1}$ . The HPBW is  $\sim 0'.7$  at 22.0 GHz. The water maser spectrum was smoothed to a resolution of  $0.3 \text{ km s}^{-1}$ .

The spectral data was processed using the GILDAS/CLASS<sup>1</sup> package. A detection was considered to be real only if its flux density was stronger than  $3\sigma$  root-mean-square (rms) noise level, the signal spanned more than three adjacent channels, and both LCP and RCP exhibited the signal. The spectra taken on different dates are co-added to measure the maser lines. Each line exhibits one or more separate groups consisting of blended components. The measurement results are presented in Table 1, where each row gives those of each group,  $\int S_v dv$  is the integrated flux density,  $V_p$  and  $S_p$  are the peak velocity and flux density, and the column titled with ‘Range’ gives the minima and maxima velocities of the group. Because most of the groups exhibit multiple blended components, we opted not to perform Gaussian fittings. The recent CO observations of I18460 suggest that the molecular gas is confined with a radius of  $0''.96$  (Khoury et al. 2021), which allows us to estimate the lower limits of the brightness temperatures ( $T_b$ ), as listed in the last column of Table 1.

### 3. RESULTS AND DISCUSSION

<sup>1</sup> See <http://www.iram.fr/IRAMFR/GILDAS> and Pety (2005).

Figure 1 shows the Stokes I (LCP+RCP) spectra of the detected masers. The spectra taken on different dates appear largely similar. We do not see any time variation in the flux and frequency of the detected features. The g-OH maser lines at 1612 and 1665 MHz are clearly detected and the intensity ratio of the 1612 and 1665 MHz lines is consistent with the properties of OH masers in typical evolved stars (Habing 1996). But that at 1667 MHz is invisible at a noise level of  $\sim 300$  mJy. Both 1612 and 1665 MHz masers exhibit two well-separated velocity components at velocities of about 110 and 140 km s<sup>-1</sup>, while the former shows several sub-features and lower-velocity components. A close inspection of Figure 1 shows that the 1665 MHz maser is slightly more extended than the 1612 MHz maser in the velocity range (see also Table 1). This behavior is opposite to that of most of the AGB envelopes, where the 1612 MHz maser originates from the outermost regions of the accelerated envelope. A possible explanation is that the inner regions may have been accelerated through the interaction with the WF jets situated within the OH shell. High spatial resolution observations and an elaborated modelling are required to clarify this.

The ex-OH masers at 4660 and 6031 MHz are unambiguously detected in the spectra of all dates. No other late-type stars exhibit so intense ex-OH masers. The 4660 MHz line arises from the  $^2 \Pi_{1/2}$ ,  $J = 2/1$ ,  $F = 0-1$  transition. The blue-shifted and red-shifted components of the 4660 MHz ex-OH maser peak at 111.4 and 138.3 km s<sup>-1</sup>, respectively, with a central velocity of about 124.9 km s<sup>-1</sup>. Both the 4660 MHz and 1612 MHz masers exhibit sub-features at the red wing of the 111.4 km s<sup>-1</sup> group and at the blue wing of the 138.3 km s<sup>-1</sup> group. We note that the interferometric observations of the molecular cloud Sgr B shows that the 4660 MHz and 1612 MHz maser spots are spatially coincident (Gardner et al. 1987). However, weak sub-features at 120–135 km s<sup>-1</sup> and 141–143 km s<sup>-1</sup> of the 1612 MHz maser are invisible in the 4660 MHz maser. The blue-shifted group of the 4660 MHz maser has a flux density of 103.4 Jy, which is much stronger than those detected in high-mass star-forming regions (HMSFR, Qiao et al. 2022). The weak 6031 MHz maser, arising from the  $^2 \Pi_{3/2}$ ,  $J = 5/2$ ,  $F = 2-2$  transition, shows only one red-shifted component peaking at 138.3 km s<sup>-1</sup> with a sharp profile. Under a local thermodynamic equilibrium condition, the intensity ratio between the 4660 MHz and the 6031 MHz lines should be  $\sim 1.5$ . However, the measured values are 38.4 and

$> 2000$  for the red-shifted and blue-shifted groups, respectively. This is apparently an indication of maser emission. Strikingly, the two main groups of the other masers behave conversely to those of the 6031 MHz maser in the relative flux.

The spectrum of the water maser is markedly different from those of OH masers. We only detect two velocity components at 116.3 and 121.4 km s<sup>-1</sup>, with latter also detected in the 1612 MHz maser. In contrast to the observations of [Deguchi et al. \(2007\)](#), it no longer exhibits an extremely broad velocity spread (as shown in the bottom panel of Figure 1). [Imai et al. \(2023\)](#) performed a recent monitor observation which showed that the high-velocity water maser components faded out until February 2023. Our observations are in line with that.

In order to rule out chances from the contamination of nearby sources, we examined the Wide-field Infrared Survey Explorer (WISE) image. As shown in Figure 2, I18460 is the only visible infrared source within the TMRT beam, and there is no other infrared pumping source. The nearest maser source is G031.213-0.180, a HMSFR lying  $\sim 12'$  away from I18460. [Qiao et al. \(2022\)](#) discovered the 4660 MHz ex-OH maser toward this source, which peaks at 111.1 km s<sup>-1</sup> and has a flux density of 0.3 Jy. Therefore, it is impossible to contaminate our detection.

The 4660 MHz ex-OH maser has a center velocity comparable to the systemic velocity obtained from the Very Long Baseline Array (124.7 km s<sup>-1</sup>, [Imai et al. 2013](#)). It is likely to originate from an expanding shell with a velocity of  $\sim 14$  km s<sup>-1</sup>, which is slightly lower than that indicated by the g-OH 1665 MHz masers ( $\sim 15$  km s<sup>-1</sup>, see Figure 1). We hypothesize that the ex-OH 4660 MHz maser may traces the high-density shocked gas which has been decelerated through the interaction between the stellar winds and the interstellar medium. A more sophisticated analysis, like that performed by [Pihlström et al. \(2008\)](#) for supernova remnants, is required to elucidate the behavior of the ex-OH masers. It is intriguing to note that the ex-OH 4660 MHz and g-OH 1665 MHz masers seem to be complementary in profile, and all their peaks can be seen in the g-OH 1612 MHz maser (Figure 1).

Previous observations of ex-OH masers toward evolved stars only reveal blue-shifted component ([Desmurs et al. 2010](#); [Strack et al. 2019](#); [Hou & Gao 2020](#)), which might be partly caused by the effect of the optical thickness. The current work is the first case of ex-OH masers being discovered

exclusively on the red-shifted side. Previous observations of ex-OH masers include the 6035 MHz in Vy 2-2 and K 3-35 (Desmurs et al. 2010) and the 4765 MHz line in CRL 618 (Strack et al. 2019). Both masers are not discovered in I18460, suggesting that the excitation of the ex-OH maser is very sensitive to the circumstellar physical conditions. We observed an asymmetry in intensity between the red- and blue-shifted groups in the 4660 MHz line, as well as in the 6031 MHz line. This phenomenon could be attributed to the spatial fluctuations of density, temperature, and velocity fields.

Extensive researches have been performed on the pumping of g-OH masers in CSEs (e.g. Thai-Q-Tung et al. 1998; Gray et al. 2005), but little is known about the pumping process of ex-OH masers. The classic model of g-OH maser in circumstellar envelope proposed by Elitzur et al. (1976) suggests that the 1612 MHz maser can be pumped from the  $^2\Pi_{1/2}$ ,  $J = 5/2$  state by infrared radiation around  $35\ \mu\text{m}$ . Elitzur (1981) suggested that infrared radiation around  $53\ \mu\text{m}$  could also contribute to the pumping of the 1612 MHz OH maser from the  $^2\Pi_{1/2}$ ,  $J = 3/2$  state, which was subsequently found to be the dominant inversion mechanism (Gray et al. 2005). Apart from that, the collisional excitation within the  $^2\Pi_{3/2}$  ladder also plays an important role on the pumping of this maser (Gray et al. 2005). Observations of ex-OH masers may shed important insight into the model. The 4660 MHz maser is pumped by infrared radiation at  $79\ \mu\text{m}$ , and its large intensity indicates that infrared pumping from  $^2\Pi_{1/2}$  significantly contributes to the inversion of the 1612 MHz g-OH maser level. The model developed for star-forming regions predicts that it is possible to simultaneously detect the two masers under the conditions of a strong far-infrared line overlap and long gain lengths (Gray et al. 1992).

The weakness of the 6031 MHz maser suggests that the collisional excitation within the  $^2\Pi_{3/2}$  ladder may be insignificant for the excitation of the 1612 MHz g-OH maser. I18460 is the only WF detected in ex-OH masers so far. However, its other properties, such as infrared luminosity and color, are not peculiar compared to other WFs. The origin of intense ex-OH masers in I18460 is unclear. Further search for ex-OH masers in WFs is desirable.

Wolak et al. (2012) did not detect the Zeeman splitting in the g-OH maser at 1665 MHz. We have attempted to examine the Zeeman splitting by comparing the LCP and RCP of the ex-OH masers at 4660 MHz and 6031 MHz. Figure 3 shows the LCP and RCP spectra of the 6031 MHz maser. They



were obtained by co-adding the spectra taken on different dates, resulting in a rms of  $\sim 50$  mJy. Gaussian fittings show that the 6031 MHz LCP and RCP lines highly coincide, and both have a peak velocity of  $138.32 \text{ km s}^{-1}$  and a width of  $0.46 \text{ km s}^{-1}$ . Therefore, we cannot detect the Zeeman splitting under the velocity resolution of  $0.07 \text{ km s}^{-1}$ . The 4660 MHz maser has a negligible Lande g-factor has thus cannot exhibit the Zeeman splitting (Gray et al. 2001). Through the observation of the 6031 MHz maser, we estimate the upper limit of the magnetic field strength to be  $\sim 0.89$  mG. Such a weak magnetic field is unlikely to contribute to the PN shaping. However, it should be cautioned that the OH shell is far away from the central engine accelerating the WF jets. Therefore, we cannot completely rule out the existence of a stronger magnetic field in the central impact region. Further interferometric observations are desirable to investigate the role of magnetic fields in PNe shaping.

#### 4. CONCLUSION

We unambiguously detected rare ex-OH masers at 4660 and 6031 MHz toward the WF source I18460 using the TMRT. To our best knowledge, this is for the first time that the ex-OH masers are discovered in a WF source and that the ex-OH maser at 4660 MHz is observed in CSEs of evolved stars. The 4660 MHz maser turns out to be abnormally strong and closely resembles the g-OH maser at 1612 MHz. The 6031 MHz maser exhibits the red-shifted component only. The puzzling behaviors of the ex-OH masers are largely unexplored, and would call for high spatial resolution observations and elaborated maser modelling.

#### ACKNOWLEDGEMENTS

We acknowledge an anonymous referee for his/her constructive comments. The financial supports of this work are from the National Science Foundation of China (NSFC, No. 12333005 and No. 11973099) and the science research grants from the China Manned Space Project (NO. CMS-CSST-2021-A09, CMS-CSST-2021-A10, etc). H.-H.Q. is supported by the Youth Innovation Promotion Association CAS and National Natural Science Foundation of China (grant No. 11903038).

#### REFERENCES

- Amiri, N., Vlemmings, W. H. T., Kemball, A. J., & van Langevelde, H. J. 2012, *A&A*, 538, A136, doi: [10.1051/0004-6361/201117452](https://doi.org/10.1051/0004-6361/201117452)
- Balick, B., Frank, A., & Liu, B. 2020, *ApJ*, 889, 13, doi: [10.3847/1538-4357/ab5651](https://doi.org/10.3847/1538-4357/ab5651)

- Claussen, M. J., & Fix, J. D. 1981, *ApJL*, 250, L77, doi: [10.1086/183677](https://doi.org/10.1086/183677)
- Cragg, D. M., Sobolev, A. M., & Godfrey, P. D. 2002, *MNRAS*, 331, 521, doi: [10.1046/j.1365-8711.2002.05226.x](https://doi.org/10.1046/j.1365-8711.2002.05226.x)
- Deguchi, S., Nakashima, J.-i., Kwok, S., & Koning, N. 2007, *ApJ*, 664, 1130, doi: [10.1086/519154](https://doi.org/10.1086/519154)
- Desmurs, J. F. 2012, in *Cosmic Masers - from OH to H0*, ed. R. S. Booth, W. H. T. Vlemmings, & E. M. L. Humphreys, Vol. 287, 217–224, doi: [10.1017/S1743921312006990](https://doi.org/10.1017/S1743921312006990)
- Desmurs, J. F., Baudry, A., Sivagnanam, P., et al. 2010, *A&A*, 520, A45, doi: [10.1051/0004-6361/200913387](https://doi.org/10.1051/0004-6361/200913387)
- Elitzur, M. 1981, in *Astrophysics and Space Science Library*, Vol. 88, *Physical Processes in Red Giants*, ed. J. Iben, I. & A. Renzini, 363–382, doi: [10.1007/978-94-009-8492-9\\_40](https://doi.org/10.1007/978-94-009-8492-9_40)
- Elitzur, M., Goldreich, P., & Scoville, N. 1976, *ApJ*, 205, 384, doi: [10.1086/154289](https://doi.org/10.1086/154289)
- Falceta-Gonçalves, D., & Jatenco-Pereira, V. 2002, *ApJ*, 576, 976, doi: [10.1086/341794](https://doi.org/10.1086/341794)
- Frank, A., & Blackman, E. G. 2004, *ApJ*, 614, 737, doi: [10.1086/382018](https://doi.org/10.1086/382018)
- Gardner, F. F., Whiteoak, J. B., & Palmer, P. 1987, *MNRAS*, 225, 469, doi: [10.1093/mnras/225.3.469](https://doi.org/10.1093/mnras/225.3.469)
- Gledhill, T. M., Chrysostomou, A., Hough, J. H., & Yates, J. A. 2001, *MNRAS*, 322, 321, doi: [10.1046/j.1365-8711.2001.04112.x](https://doi.org/10.1046/j.1365-8711.2001.04112.x)
- Gómez, J. F., Rizzo, J. R., Suárez, O., et al. 2011, *ApJL*, 739, L14, doi: [10.1088/2041-8205/739/1/L14](https://doi.org/10.1088/2041-8205/739/1/L14)
- Gómez, J. F., Suárez, O., Rizzo, J. R., et al. 2017, *MNRAS*, 468, 2081, doi: [10.1093/mnras/stx650](https://doi.org/10.1093/mnras/stx650)
- Gómez, J. F., Uscanga, L., Green, J. A., et al. 2016, *MNRAS*, 461, 3259, doi: [10.1093/mnras/stw1536](https://doi.org/10.1093/mnras/stw1536)
- Gray, M. D., Cohen, R. J., Richards, A. M. S., Yates, J. A., & Field, D. 2001, *MNRAS*, 324, 643, doi: [10.1046/j.1365-8711.2001.04349.x](https://doi.org/10.1046/j.1365-8711.2001.04349.x)
- Gray, M. D., Field, D., & Doel, R. C. 1992, *A&A*, 262, 555
- Gray, M. D., Howe, D. A., & Lewis, B. M. 2005, *MNRAS*, 364, 783, doi: [10.1111/j.1365-2966.2005.09591.x](https://doi.org/10.1111/j.1365-2966.2005.09591.x)
- Habing, H. J. 1996, *A&A Rv*, 7, 97, doi: [10.1007/PL00013287](https://doi.org/10.1007/PL00013287)
- Herman, J., Baud, B., & Habing, H. J. 1985, *A&A*, 144, 514
- Hou, L. G., & Gao, X. Y. 2020, *MNRAS*, 495, 4326, doi: [10.1093/mnras/staa1461](https://doi.org/10.1093/mnras/staa1461)
- Imai, H. 2007, in *Astrophysical Masers and their Environments*, ed. J. M. Chapman & W. A. Baan, Vol. 242, 279–286, doi: [10.1017/S1743921307013130](https://doi.org/10.1017/S1743921307013130)
- Imai, H., Deguchi, S., Nakashima, J.-i., Kwok, S., & Diamond, P. J. 2013, *ApJ*, 773, 182, doi: [10.1088/0004-637X/773/2/182](https://doi.org/10.1088/0004-637X/773/2/182)
- Imai, H., Uno, Y., Maeyama, D., et al. 2020, *PASJ*, 72, 58, doi: [10.1093/pasj/psaa047](https://doi.org/10.1093/pasj/psaa047)

- Imai, H., Hamae, Y., Amada, K., et al. 2023, PASJ, 75, 1183, doi: [10.1093/pasj/psad064](https://doi.org/10.1093/pasj/psad064)
- Khourri, T., Vlemmings, W. H. T., Tafuya, D., et al. 2021, Nature Astronomy, 6, 275, doi: [10.1038/s41550-021-01528-4](https://doi.org/10.1038/s41550-021-01528-4)
- Kwok, S. 1993, ARA&A, 31, 63, doi: [10.1146/annurev.aa.31.090193.000431](https://doi.org/10.1146/annurev.aa.31.090193.000431)
- Li, J., Shen, Z.-Q., Wang, J., et al. 2016, ApJ, 824, 136, doi: [10.3847/0004-637X/824/2/136](https://doi.org/10.3847/0004-637X/824/2/136)
- Livio, M., & Soker, N. 1988, ApJ, 329, 764, doi: [10.1086/166419](https://doi.org/10.1086/166419)
- Nordhaus, J., & Blackman, E. G. 2006, MNRAS, 370, 2004, doi: [10.1111/j.1365-2966.2006.10625.x](https://doi.org/10.1111/j.1365-2966.2006.10625.x)
- Pety, J. 2005, in SF2A-2005: Semaine de l’Astrophysique Francaise, ed. F. Casoli, T. Contini, J. M. Hameury, & L. Pagani, 721
- Pihlström, Y. M., Fish, V. L., Sjouwerman, L. O., et al. 2008, ApJ, 676, 371, doi: [10.1086/529009](https://doi.org/10.1086/529009)
- Qiao, H.-H., Shen, Z.-Q., Breen, S. L., et al. 2022, ApJ, 928, 129, doi: [10.3847/1538-4357/ac5820](https://doi.org/10.3847/1538-4357/ac5820)
- Rizzo, J. R., Gómez, J. F., Miranda, L. F., et al. 2013, A&A, 560, A82, doi: [10.1051/0004-6361/201322187](https://doi.org/10.1051/0004-6361/201322187)
- Sahai, R., & Trauger, J. T. 1998, AJ, 116, 1357, doi: [10.1086/300504](https://doi.org/10.1086/300504)
- Sevenster, M. N., Chapman, J. M., Habing, H. J., Killeen, N. E. B., & Lindqvist, M. 1997, A&AS, 124, 509, doi: [10.1051/aas:1997365](https://doi.org/10.1051/aas:1997365)
- Sjouwerman, L. O., Fish, V. L., Claussen, M. J., Pihlström, Y. M., & Zschaechner, L. K. 2007, ApJL, 666, L101, doi: [10.1086/521827](https://doi.org/10.1086/521827)
- Strack, A., Araya, E. D., Lebrón, M. E., et al. 2019, ApJ, 878, 90, doi: [10.3847/1538-4357/ab1f93](https://doi.org/10.3847/1538-4357/ab1f93)
- Suárez, O., Gómez, J. F., & Miranda, L. F. 2008, ApJ, 689, 430, doi: [10.1086/592493](https://doi.org/10.1086/592493)
- Tafuya, D., Imai, H., Gómez, J. F., et al. 2020, ApJL, 890, L14, doi: [10.3847/2041-8213/ab70b8](https://doi.org/10.3847/2041-8213/ab70b8)
- Thai-Q-Tung, Dinh-v-Trung, Nguyen-Q-Rieu, et al. 1998, A&A, 331, 317
- Tocknell, J., De Marco, O., & Wardle, M. 2014, MNRAS, 439, 2014, doi: [10.1093/mnras/stu079](https://doi.org/10.1093/mnras/stu079)
- Ueta, T., Meixner, M., & Bobrowsky, M. 2000, ApJ, 528, 861, doi: [10.1086/308208](https://doi.org/10.1086/308208)
- Uscanga, L., Imai, H., Gómez, J. F., et al. 2023, ApJ, 948, 17, doi: [10.3847/1538-4357/acc06f](https://doi.org/10.3847/1538-4357/acc06f)
- Vlemmings, W. H. T. 2014, in Magnetic Fields throughout Stellar Evolution, ed. P. Petit, M. Jardine, & H. C. Spruit, Vol. 302, 389–397, doi: [10.1017/S1743921314002580](https://doi.org/10.1017/S1743921314002580)
- Wardle, M. 2007, in Astrophysical Masers and their Environments, ed. J. M. Chapman & W. A. Baan, Vol. 242, 336–337, doi: [10.1017/S1743921307013300](https://doi.org/10.1017/S1743921307013300)
- Wolak, P., Szymczak, M., & Gérard, E. 2012, A&A, 537, A5, doi: [10.1051/0004-6361/201117263](https://doi.org/10.1051/0004-6361/201117263)
- Zuckerman, B., Yen, J. L., Gottlieb, C. A., & Palmer, P. 1972, ApJ, 177, 59, doi: [10.1086/151686](https://doi.org/10.1086/151686)

**Table 1.** Measurements of masers in I18460.

Frequency	$\int S_v dv$	$V_p$	Range	$S_p$	rms	$T_b$
(MHz)	(Jy km s <sup>-1</sup> )	(km s <sup>-1</sup> )	(km s <sup>-1</sup> )	(Jy)	(Jy)	(10 <sup>5</sup> K)
(1)	(2)	(3)	(4)	(5)	(6)	(7)
1612	171.14	111.1	110.0, 114.5	123.42	0.39	> 629.77
1612	10.36	121.1	119.0, 124.0	6.82	0.39	> 34.80
1612	59.74	138.4	135.8, 142.8	28.20	0.39	> 143.90
1665	8.86	110.4	109.0, 111.3	20.36	0.50	> 97.38
1665	4.98	140.4	139.2, 142.6	4.22	0.50	> 20.18
4660	117.86	111.4	109.8, 117.7	103.40	0.16	> 63.14
4660	22.98	138.3	135.8, 140.7	19.96	0.16	> 12.19
6031	0.18	138.4	137.8, 138.9	0.52	0.09	> 0.19
22235	1.58	116.3	114.9, 117.3	2.54	0.39	> 0.07
22235	3.98	121.4	120.2, 123.3	4.70	0.39	> 0.13

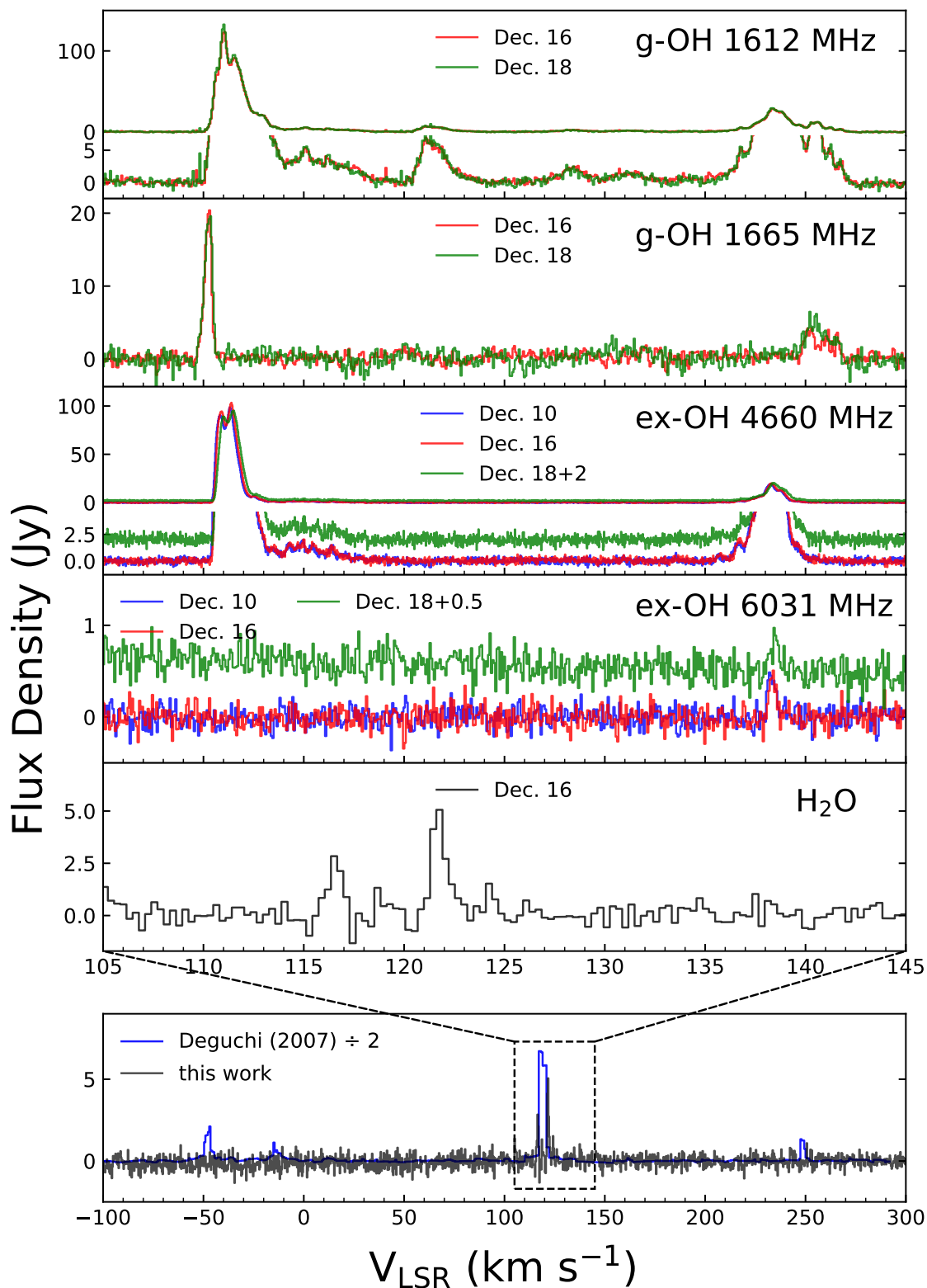


**Figure 1.** The maser spectra of I18460 after subtracting the baseline. The flux density is shown for the Stokes I (LCP+RCP). In each panel, the colorful curves represent the spectra taken on different dates. Zoom-in views are provided below the spectra of the 1612 and 4660 lines. The bottom panel compares the water maser line observed in this work and that by Deguchi et al. (2007) in a broader velocity range.

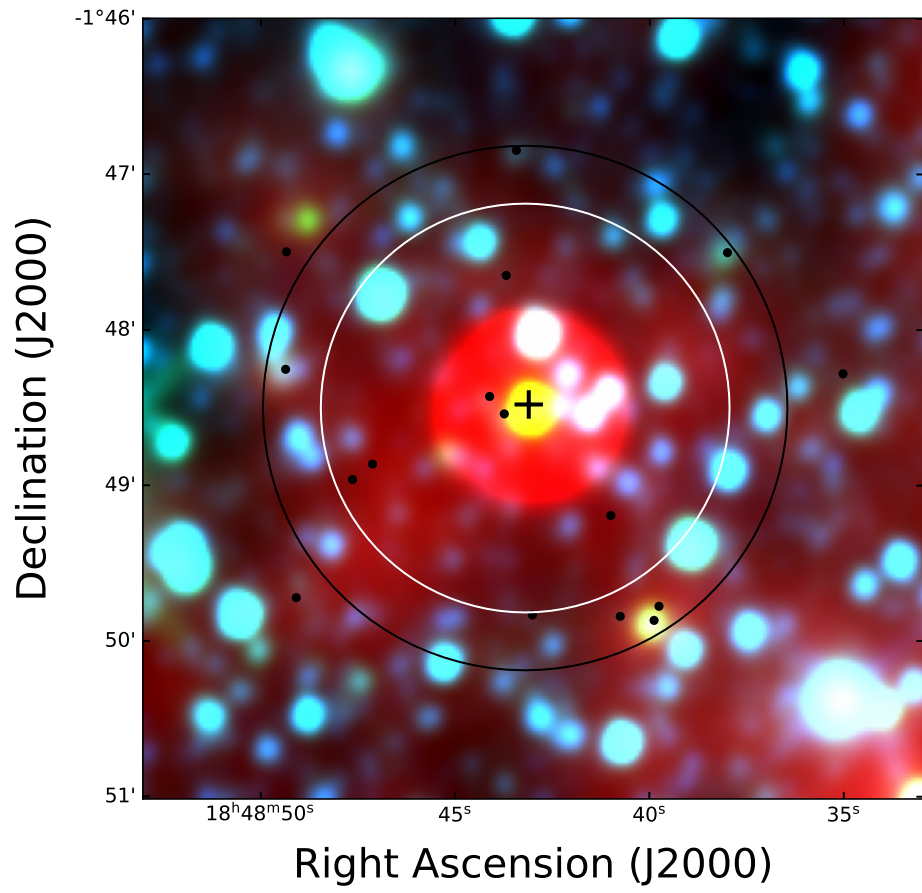


**Figure 2.** The WISE image of I18460. The 3.4, 4.6, and 22  $\mu\text{m}$  bands are shown in blue, green, and red, respectively. The white and black circles indicate the beam sizes of TMRT at 6.0 and 4.7 GHz, respectively, and the cross marks the position of the beam center. The dots denote the surrounding young stellar objects.

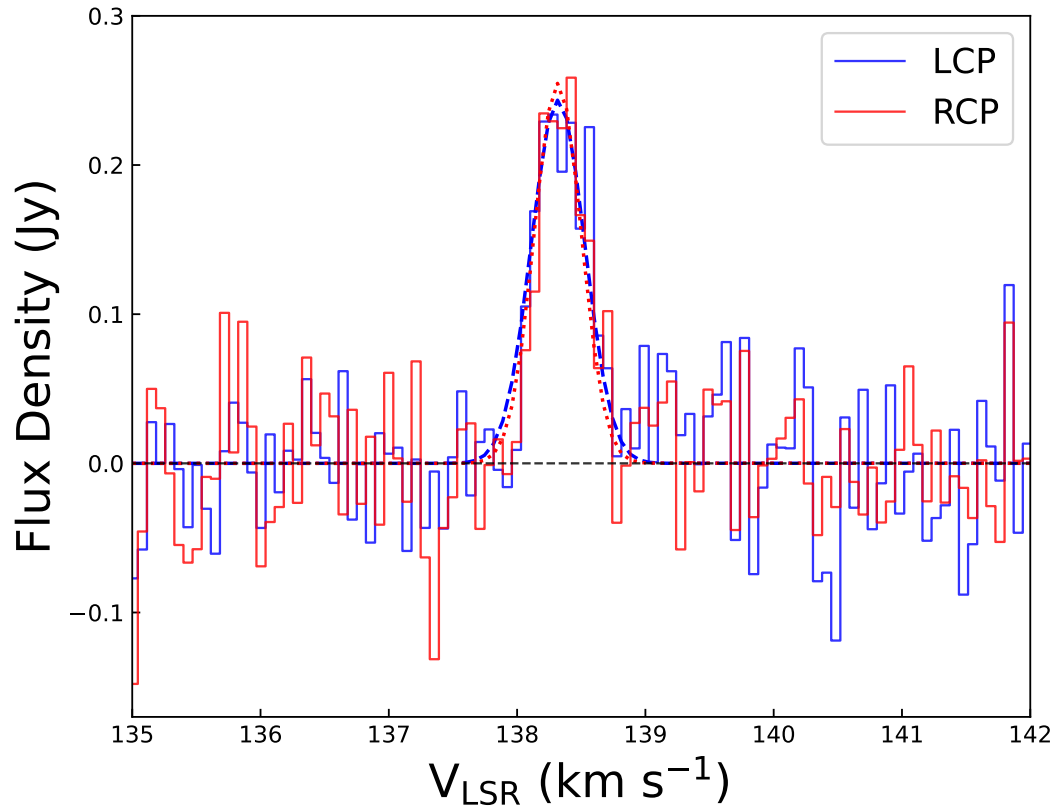


**Figure 3.** Circular polarization spectra of the 6031 MHz OH maser. The stepped and dashed curves represent the observations and Gaussian fittings, respectively.